Journal of Applied Sciences 8 (21): 3806-3816, 2008
ISSN 1812-5654

Multidimensional Combustion Simulation and Analytical Solution of Wall Heat Conduction in DI Diesel Engine

M.H. Djavareshkian, F. Talati, A. Ghasemi and S. Sohrabi
Department of Mechanical Engineering, University of Tabriz, Tabriz, Iran

Abstract: In this research, combustion process in the combustion chamber of a DI diesel engine is simulated. Afterwards, results obtained from the multidimensional simulation of the combustion process are used in analytical solution of the heat conduction in cylinder wall. An eddy break-up combustion model and a diesel auto-ignition model were implemented to simulate the ignition and combustion process. All the simulations were carried out by the use of FIRE CFD tool. Numerical results were validated via experimental data for OM_355 DI diesel engine for mean cylinder pressure. The results show that there have been good agreements between experimental data and the CFD calculations. The research demonstrated that the combination of multidimensional CFD simulation and analytical methods is useful for diesel engine wall heat transfer modeling. Effect of cylinder wall material, insulation material and thickness were studied in order to obtain lower heat rejection from the combustion chamber. Using cast iron instead of alluminium for cylinder material, using insulation and increasing the insulation thickness resulted in lower outer wall temperature and heat flux.

Key words: Diesel engine, ignition, combustion, heat conduction

INTRODUCTION

Heat transfer through the cylinder side walls is an important process in determining overall performance, size and cooling capacity of an Internal Combustion Engine (ICE). It affects the indicated efficiency because it reduces the cylinder temperature and pressure and thereby decreasing the work transferred on the piston per cycle. The heat loss (transfer) through the walls is in the range of 10-15% of the total fuel energy supplied to the engine during one working cycle (Sanli *et al*., 2008). During the last decades results from various theoretical and experimental researches have been presented in the literature on this subject (Rakopoulos and Mavropoulos, 2008; Mohammadi *et al*., 2008; Torregrosa, 2006).

Heat transfer in internal combustion engines is extremely complex, since the relevant phenomena are transient, three-dimensional and subject to rapid oscillations in cylinder gas pressure and temperatures, while the moving boundaries of the combustion chamber add more to this complexity (Rakopoulos *et al*., 2004a). In recent years, the interest for the heat transfer phenomena in internal combustion engines has been greatly intensified, because of their major importance, among other aspects, on successful simulations of thermodynamic cycles and investigations of thermal loading at critical places in the combustion chamber components (Rakopoulos *et al*., 2004b).

Cylinder wall insulation is an interesting design parameter of the engine cylinder, which has been dealt with in the past mainly as regards heat transfer, flow and thermal shock calculations. (Rakopoulos *et al*., 2004a).

A two-dimensional transient Heat Conduction in Components code (HCC) was successfully set up and extensively used to calculate the temperature field existing in real engine combustion chambers. In order to obtain the temperature distribution on the chamber surfaces a method needed to be developed to calculate the temperature distribution on the chamber surfaces with the aid of basic heat conduction equations. The Saul'yev method, an explicit, unconditionally stable finite difference method, was used in the code. The KIVA-II code provided the instantaneous local heat flux on the combustion chamber surfaces and the HCC code computed the time-averaged wall temperature distribution on the surfaces. If material property data and appropriate coolant-side boundary conditions are available, obtaining satisfactory combustion chamber surface temperature distributions with this method will be possible (Liu and Reitz, 1997).

Objective of this research is to utilize a multidimensional combustion model accompanied by an analytical approach to investigate cylinder wall heat conduction. For this purpose, combustion process is simulated by the use of FIRE CFD tool to give mean inner wall temperature variation with crank angle degree to be

Corresponding Author: M.H. Djavareshkian, Department of Mechanical Engineering, University of Tabriz, Tabriz, Postal Code 51666-14766, East Azerbaijan, Iran Tel: +98-914-3135532 Fax: +98-411-3354153

used as inner wall boundary condition in Duhamel's method. Numerical results were validated via experimental data for OM_355 DI diesel engine for mean cylinder pressure. Diagrams will be given to show how, the cylinder material, the insulation material and thickness, Affect the heat flux to the outer walls, the variation of cylinder temperature with cylinder depth and time in crank angle degree.

MATERIALS AND METHODS

Here, CFD simulation and analytical approach formulation are described:

COMPUTATIONAL FLUID DYNAMICS SIMULATION

Basic equations: The conservation equations are presented for the following dynamic and thermodynamic properties (FIRE v8.5 Manuals):

- Mass → equation of continuity

$$\frac{\partial \rho}{\partial t} = -\frac{\partial}{\partial x_j}\left(\rho U_j\right) \tag{1}$$

- Momentum (Newton's 2nd law) → Navier-Stokes equations

$$\begin{aligned}\frac{D(\rho U)}{Dt} &= \frac{\partial(\rho U_i)}{\partial t} + \frac{\partial(\rho U_j U_i)}{\partial x_j} \\ &= \rho g_i - \frac{\partial P}{\partial x_i} + \frac{\partial}{\partial x_j}\left[\mu\left(\frac{\partial U_i}{\partial x_j} + \frac{\partial U_j}{\partial x_i} - \frac{2}{3}\frac{\partial U_k}{\partial x_k}\delta_{ij}\right)\right]\end{aligned} \tag{2}$$

- Energy (1st law of Thermodynamics) → equation of energy

$$\begin{aligned}\frac{D(\rho H)}{Dt} &= \frac{\partial(\rho H)}{\partial t} + \frac{\partial(\rho U_j H)}{\partial x_j} \\ &= \rho \dot{q}_g + \frac{\partial P}{\partial t} + \frac{\partial}{\partial x_i}\left(\tau_{ij} U_j\right) + \frac{\partial}{\partial x_j}\left(\lambda \frac{\partial T}{\partial x_j}\right)\end{aligned} \tag{3}$$

- Concentration of species equation

$$\begin{aligned}\frac{D(\rho C)}{Dt} &= \frac{\partial(\rho C)}{\partial t} + \frac{\partial(\rho U_j C)}{\partial x_j} \\ &= \rho \dot{r} + \frac{\partial P}{\partial t} + \frac{\partial}{\partial x_j}\left(D\frac{\partial C}{\partial x_j}\right)\end{aligned} \tag{4}$$

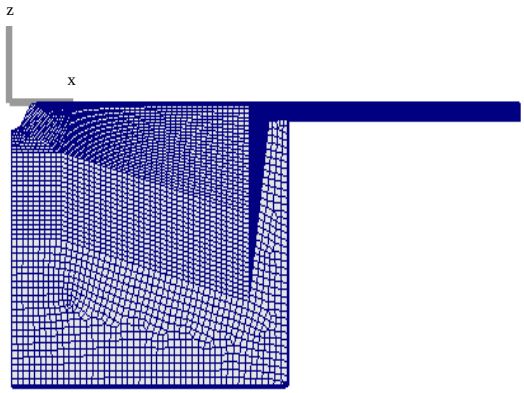

Fig. 1: Two-dimensional grid of the modeled engine

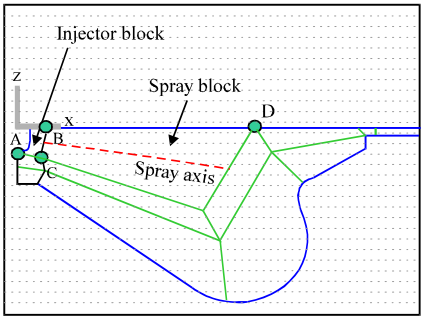

Fig. 2: Multi-block structure of the grid

Computational grid generation: Based on the geometry description, a set of computational meshes covering 360°CA is created. The mesh generation process is divided into the creation of 2D and 3D mesh. The 2D mesh of the modeled engine is shown in Fig. 1. A 90 degree sector mesh was used in this study considering that the diesel injector has four nozzle holes. This mesh resolution has been found to provide adequately independent grid results. The multi-block structure of the grid, containing spray and injector blocks, is shown in Fig. 2.

Overview of typical boundary conditions: The wall (surface) temperatures (cylinder liner, cylinder head and piston crown) are based on experimental experiences and depend on the operating point (load and speed). The boundary conditions of the cylinder head are specified as fixed wall, the boundary conditions of the piston bowl as moving wall. In Fig. 3, overview of the selected boundary conditions is shown.

Symmetry boundary conditions are applied to the radius surface along the center axis of the segment mesh. This symmetry boundary conditions might cause problems with calculation results regarding temperature. In this case adiabatic fixed wall boundary conditions can be specified. In Fig. 4, details of the boundary conditions is shown.

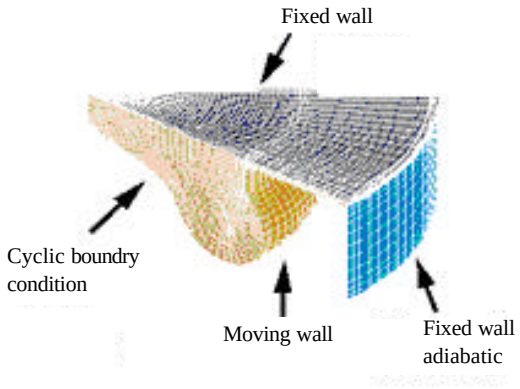

Fig. 3: Boundary conditions-overview

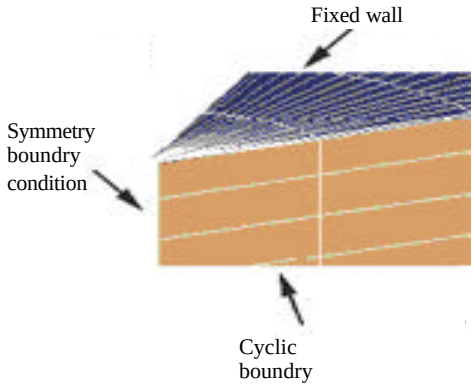

Fig. 4: Boundary conditions-details

The boundary conditions concerning the additional compensation volume are applied in this way. Faces at the outer, inner and lower side of the volume are specified as moving wall adiabatic (heat flux = 0). Figure 5 shows the moving wall adiabatic boundary conditions.

The faces in polar direction are specified as cyclic boundary conditions. Figure 6 shows selections for cyclic boundary conditions.

Model formulation: The AVL FIREv8.5 CFD tool was implemented to simulate diesel engine combustion. FIRE solves unsteady compressible turbulent reacting flows by using finite volume method. Turbulent flow in the combustion chamber was modeled with k−ε turbulence model. An eddy break-up combustion model was implemented to simulate the combustion process in a diesel engine. The reaction mechanism used for the simulation of the auto-ignition of the diesel fuel is based upon an extended version of the well known SHELL model.

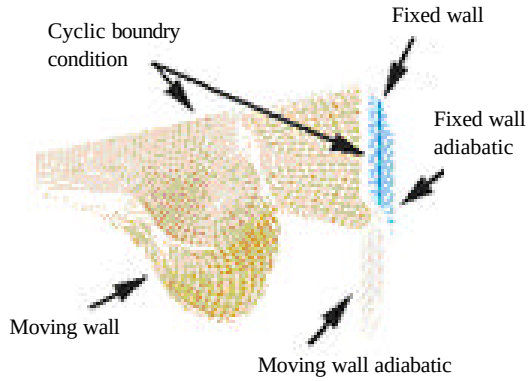

Fig. 5: Moving wall adiabatic boundary conditions

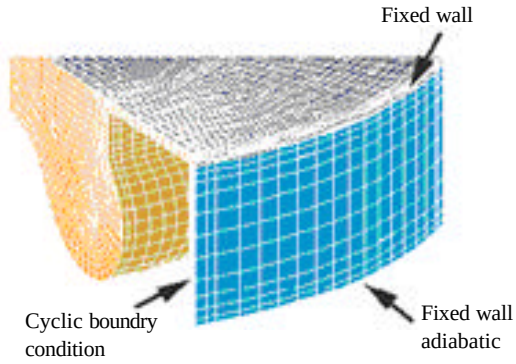

Fig. 6: Selections for cyclic boundary conditions

Auto-ignition model: The SHELL ignition model (Baumgarten, 2006) was implemented as the auto-ignition model in this study. The model uses a simplified reaction mechanism to simulate the auto-ignition of hydrocarbon fuels. The mechanism consists of eight generic reactions and five generic species. The reactions represent four types of elementary reaction steps that occur during ignition, namely, initiation, propagation, branching and termination. The five generic species include fuel, oxygen, radicals, intermediates species and branching agents. These reactions are based on the degenerate branching characteristics of hydrocarbon fuels. The premise is that degenerative branching controls the two-stage ignition and cool flame phenomena seen during hydrocarbon auto-ignition. A chain propagation cycle is formulated to describe the history of the branching agent together with one initiation and two termination reactions.

This model has been successfully applied in diesel ignition studies. It has been found that the rate-limiting step in the kinetic path is the formation of the intermediate species and the ignition delay predictions are sensitive to the pre-exponential factor A_{fi} in the rate constant of this reaction. Therefore, the above kinetic constant is adjusted to account for fuel effects.

Combustion model: The EBU model (Brink *et al*., 2000), has been developed assuming that in most technical applications the chemical reaction rates are fast compared to the mixing. Thus, the reaction rate is determined by the rate of intermixing of fuel and oxygen-containing eddies, i.e., by dissipation rate of the eddies. For such a case, the EBU model can be written:

$$\omega = A\frac{\varepsilon}{k}\min\left(Y_{fuel}, \frac{Y_{oxygen}}{r_f}, B\frac{Y_{products}}{1+r_f}\right) \quad (5)$$

where, Y is the mass fraction and r_f the stoichiometric coefficient for the overall reaction written on mass basis. A and B are experimentally determined constants of the model, whereas k is the turbulent kinetic energy and ε its dissipation rate. The product dependence for the reaction rate is a deviation from the pure fast chemistry assumption, since the assumption here is that without products the temperature will be too low for reactions. This model assumes that in premixed turbulent flames, the reactants (fuel and oxygen) are contained in the same eddies and are separated from eddies containing hot combustion products. The chemical reactions usually have time scales that are very short compared to the characteristics of the turbulent transport processes. Thus, it can be assumed that the rate of combustion is determined by the rate of intermixing on a molecular scale of eddies containing reactants and those containing hot products, in other words by the rate of dissipation of these eddies. The attractive feature of this model is that it does not call for predictions of fluctuations of reacting species (FIRE v8.5 Manuals).

Spray and break-up modeling: Currently the most common spray description is based on the Lagrangian discrete droplet method (Burger *et al*., 2002). While the continuous gaseous phase is described by the standard Eulerian conservation equations, the transport of the dispersed phase is calculated by tracking the trajectories of a certain number of representative parcels (particles). A parcel consists of a number of droplets and it is assumed that all the droplets within one parcel have the same Physical properties and behave equally when they move, break-up, hit a wall or evaporate. The coupling between the liquid and the gaseous phases is achieved by source term exchange for mass, momentum, energy and turbulence. Various sub-models were used to account for the effects of turbulent dispersion (Barata, 2008), coalescence (Post and Abraham, 2002), evaporation (Baumgarten, 2006), wall interaction (Andreassi *et al*., 2007) and droplet break up (Liu *et al*., 2008).

ANALYTICAL APPROACH FORMULATION

Heat transfer rate from gas to cylinder wall is a harmonic function of time; therefore a Fourier series analytical solution was implemented. For simplification it was assumed that there is a uniform temperature distribution on inner side of cylinder wall. Heat conduction through the cylinder wall was considered to be one dimensional, this sounds reasonable because there is a faster variation of the temperature in a direction normal to the wall surface. In order to calculate the heat transfer rate, from IVC to EVO, transient equation of heat conduction is solved using appropriate boundary conditions. Total temperature, T(r, t), which contains steady and periodic temperature terms, must satisfy one dimensional heat conduction equation in each time t and for all positions r:

$$\frac{\partial T}{\partial t} = \alpha\frac{\partial^2 T}{\partial^2 r} \quad (6)$$

where, α is the thermal diffusivity coefficient. Equation 6 is solved by being separated into steady and transient parts.

Steady heat conduction problem: Because of the greater cylinder diameter compared with its thickness it can be considered as a slab. In this model outer wall temperature, T_c (is approximately equal to mean coolant fluid temperature) is known. Thus steady equation of temperature distribution through a wall with a thickness of $l_w = r_{outer} - r_{inner}$ is:

$$T_{mx} = T_{mw} - \left(\frac{r - r_{inner}}{L_w}\right)(T_{mw} - T_c) \quad (7)$$

In Eq. 7, T_{mw} is the mean inner wall temperature extracted from CFD simulation of the combustion.

Periodic heat conduction problem: Periodic term of the temperature, T_p (r, t), must satisfy the following equation in each time t and for all positions r:

$$\frac{\partial T_p}{\partial t} = \alpha\frac{\partial^2 T_p}{\partial r^2} \quad (8)$$

Equation 8 is solved analytically by using Fourier technique. The boundary conditions are as follows:

$$\begin{cases} T = T_W(t) & \text{at } r = r_{inner} \\ T = T_l & \text{at } r = r_{outer} \end{cases} \quad (9)$$

In steady engine operation, mean inner wall temperature is a periodic function in the calculation domain (from IVC to EVO). So, it can be written as a Fourier series:

$$T_w = T_m + \sum_{n=1}^{N}[A_n \cos(n\omega t) + B_n \sin(n\omega t)] \quad (10)$$

where, T_m is the time averaged term, A_n and B_n are the Fourier coefficients, n is a harmonic and ω is angular frequency. The coefficients may be calculated by the following formulas:

$$A_0 = T_m = \frac{1}{\tau_0}\int_0^{\tau_0} T_w(t)\,dt \quad (11)$$

$$A_n = \frac{2}{\tau_0}\int_0^{\tau_0} T_w(t)\cos(\frac{2\pi n}{\tau_0}t)dt \quad (12)$$

$$B_n = \frac{2}{\tau_0}\int_0^{\tau_0} T_w(t)\mathrm{Sin}(\frac{2\pi n}{\tau_0}t)dt \quad (13)$$

Now temperature can be written in exponential form:

$$T(r,t) = T_m - (T_m - T_l)\frac{r - r_{inner}}{l} + \sum_{n=1}^{N}\exp(-\phi_n(r - r_{inner}))F_n(x,t) \quad (14)$$

Where:

$$F_n = A_n \cos\left(n\omega t - \phi_n(r - r_{inner})\right) + B_n \sin\left(n\omega t - \phi_n(r - r_{inner})\right) \quad (15)$$

And

$$\phi_n = (\frac{n\omega}{2\alpha})^{0.5}$$

Now having the temperature distribution enables us to easily calculate the heat flux by the use of Fourier law:

$$\dot{q}_w = \dot{q}_{mr} + \dot{q}_p = \frac{\lambda}{l}(T_m - Tn_l) + \lambda\sum_{n=1}^{N}\phi_n[(A_n + B_n)\cos(n\omega t) - (A_n - B_n)\sin(n\omega t)] \quad (16)$$

ENGINE SPECIFICATIONS, OPERATING CONDITIONS AND INVESTIGATED CASES

The OM_355 Mercedes Benz diesel engine is used in this simulation. The specifications of mentioned engine are shown in Table 1.

Table 1: OM-355 engine specifications and operating conditions

Engine model	OM-355	SOI (ATDC)	-18.500
No. of cylinders	6	Inlet air temp. (K)	300.000
Bore	128 (mm)	Inlet air press. (kPa)	99.000
Stroke	150 (mm)	ϕ_{diesel}	0.789
Compression ratio	16.1:1		
Maximum torque speed	1400 (rpm)		

Table 2: Different cases defined to study

Case	Chamber wall material	Wall thickness (mm)	Insulation thickness (mm)
1	Cast iron	10.0	-
2	Alluminium	10.0	-
3	Cast iron+Ins1	9.5	0.5
4	Cast iron+Ins1	9.0	1.0
5	Cast iron+Ins2	9.5	0.5
6	Cast iron+Ins2	9.0	1.0

Table 3: Physical properties of the different materials used (Heywood, 1988)

Material	Thermal conductivity (λ) W mK^{-1}	Density (ρ) kg m^{-3}	Specific heat (c) J $kg.K^{-1}$	Thermal diffusivity (α) m^2 sec^{-1}
Cast iron	54	7.2×10^3	480	1.57×10^{-5}
Alluminium	155	2.75×10^3	915	6.20×10^{-5}
Ins1 (Reaction-bonded silicon nitride)	10	2.5×10^3	710	2.80×10^{-6}
Ins2 (Sprayed zirconia)	1.2	5.2×10^3	732	3.20×10^{-7}

Equation 17 shows how the equivalence ratio in Table 1 is calculated. Table 2 shows the different cases defined to study. Table 3 shows the physical properties of the different materials (Heywood, 1988).

$$\phi_{diesel} = \frac{(AFR)_{st}}{(AFR)_{act}} \quad (17)$$

RESULTS AND DISCUSSION

Here, the results of the diesel combustion simulation are discussed first and later the analytical results of the wall heat conduction are talked over. In the analytical part effects of the cylinder wall material, insulation material and thickness are argued.

Results of the diesel combustion simulation: Figure 7 shows the comparison of mean cylinder pressure for present calculation and experimental data (Pirouzpanah *et al.*, 2003). As it can be seen, the agreement between two results is very good.

Figure 8 shows the variations of mean cylinder temperature with crank angle.

Figure 9 exhibits diesel combustion behavior containing premixed and diffusion stages of combustion. Comparing this diagram with temperature and pressure diagrams shows high rates of temperature and pressure rise during the premixed combustion period.

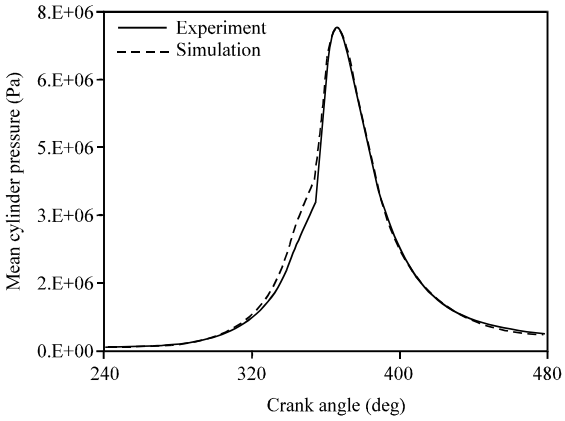

Fig. 7: Comparison of cylinder pressure for Model and experiment (Pirouzpanah *et al.*, 2003)

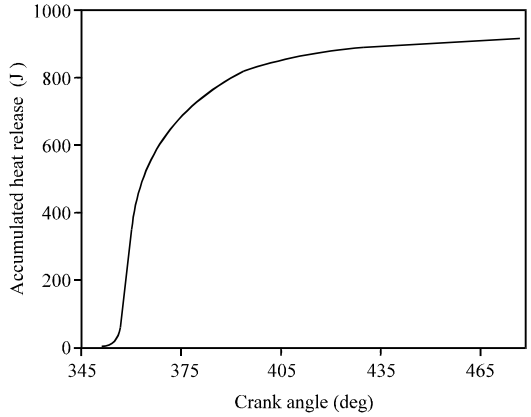

Fig. 10: Accumulated heat release

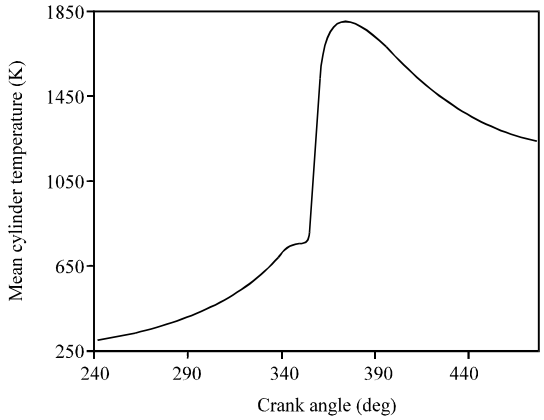

Fig. 8: Variations of mean cylinder temperature with crank angle

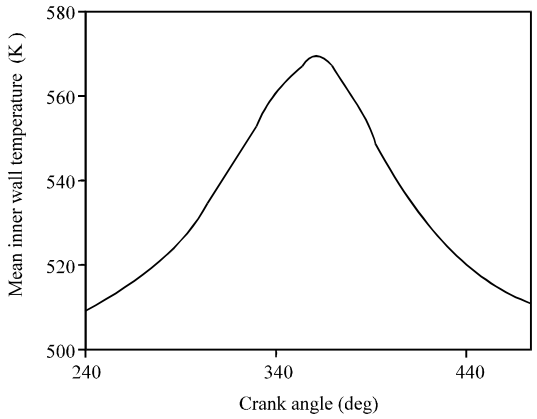

Fig. 11: Mean inner wall temperature

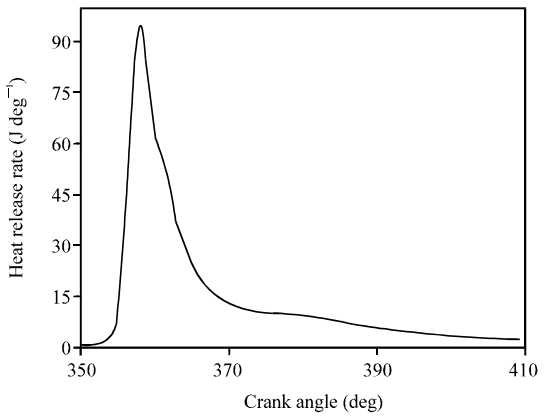

Fig. 9: Heat release rate diagram

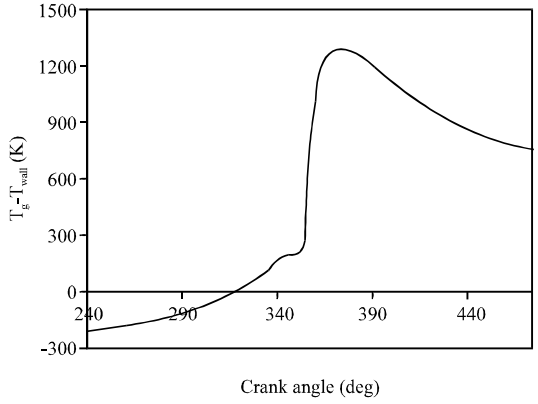

Fig. 12: Mean temperature difference between cylinder gas and inner wall surface

Figure 10 shows the accumulated heat released in diesel combustion. In Fig. 11 and 12 mean inner wall temperature and mean temperature difference between cylinder gas and inner wall surface are demonstrated. The mean inner wall temperature was used as boundary

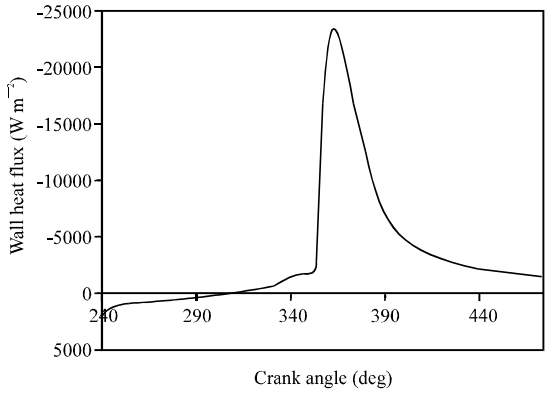

Fig. 13: Wall heat flux

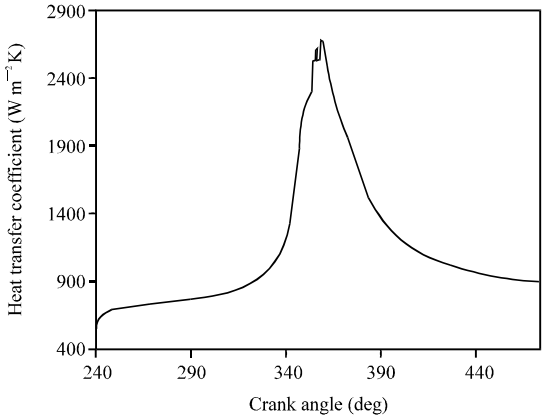

Fig. 14: Near wall temperature based heat transfer coefficient

condition for analytical procedure. By comparing Fig. 12 and 13, which shows the variation of wall heat flux, it can be drawn that ($T_{gas}-T_{wall}$), has its minimum values and this is accompanied by the lowest levels of heat flux, in crank angles from about 310 to 330.

Figure 14 shows the near wall temperature based heat transfer coefficient; comparing this graph to Fig. 13 shows that in crank angles between about 360-365, higher heat transfer coefficients comes along with greater values of heat rejection out of the in cylinder control volume.

Results of the analytical solution: In the following diagrams results obtained from analytical solution of heat conduction in cylinder wall are discussed. $x = r-r_{inner}$ is the penetration depth in the cylinder wall.

Effect of cylinder wall material on temperature distribution (cases 1 and 2): Figure 15-19 show the variations of wall temperature vs crank angle and position for cases 1 and 2. It can be seen that in the diagrams of

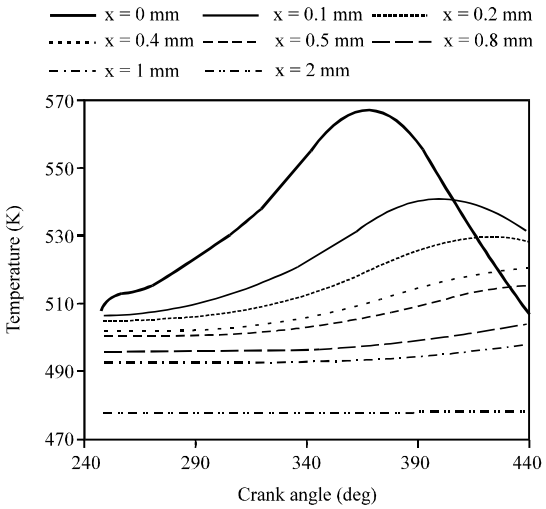

Fig. 15: Variation of wall temperature vs crank angle for different cylinder wall depth in case 1

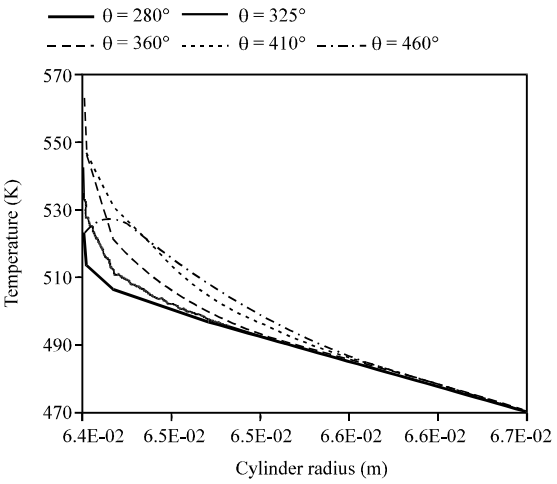

Fig. 16: Variation of wall temperature vs cylinder wall depth for different crank angles in case 1

temperature vs. crank angle, increase in depth leads to a fall off and delay in temperature peak and that is because of the reduction of temperature oscillation with depth. In the diagrams of temperature vs. depth, increase in depth is along with damping of temperature oscillations after and it seems that temperature graphs come together after a distance. Because of the lower thermal diffusivity, this distance is smaller for case 1 in comparison with case 2. Another important behavior to be mentioned is that, temperature decreases with depth up to TDC, but after this time it increases first and then decreases with depth. In another words before TDC position, maximum temperature occurs on inner wall surface but after that it is somewhere inside the wall.

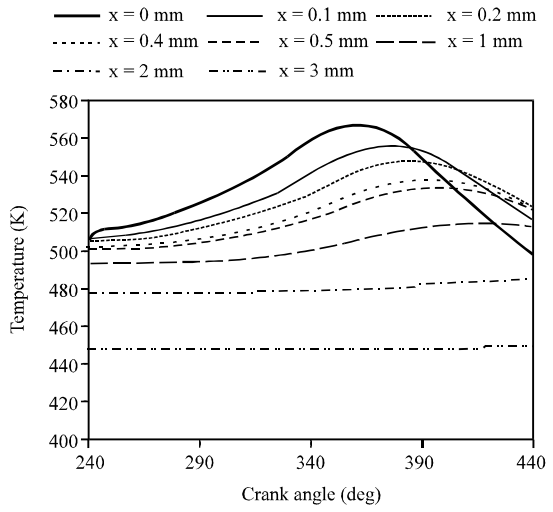

Fig. 17: Variation of wall temperature vs crank angle for different cylinder wall depth in case 2

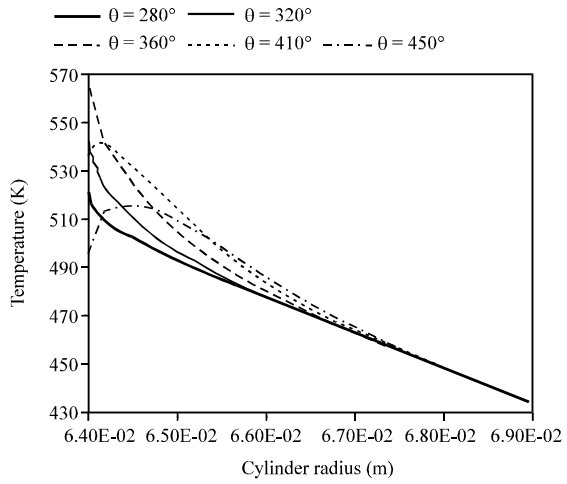

Fig. 18: Variation of wall temperature vs cylinder wall depth for different crank angles in case 2

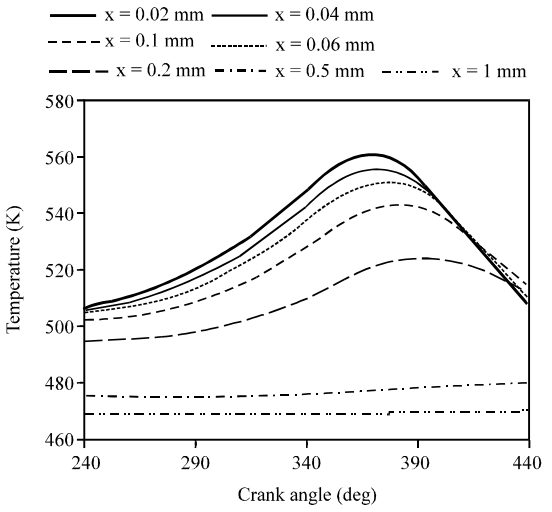

Fig. 19: Variation of wall temperature vs crank angle for different cylinder wall depth in case 3

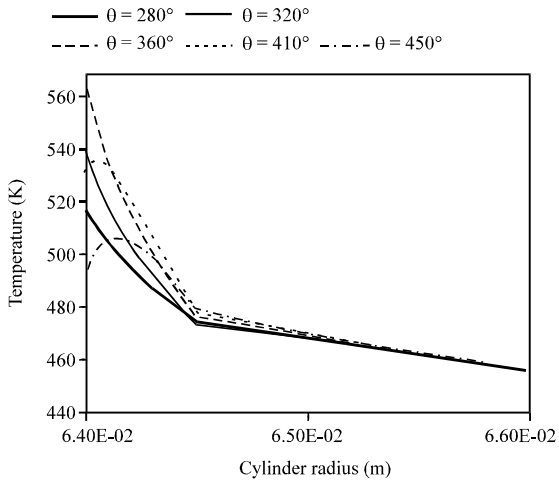

Fig. 20: Variation of wall temperature vs cylinder wall depth for different crank angles in case 3

Effect of insulation material and thickness on temperature distribution (cases 3-6): Here, effect of insulation material and thickness on temperature distribution is investigated. Figure 18-26 show the variations of wall temperature vs crank angle and position for cases 3-6. Comparing Fig. 19 and 21 shows that increasing the insulation thickness results in lower outer wall temperature. There is a breakage in temperature graph, at the boundary face between the insulation and the cylinder wall in Fig. 20 and 22. That is because of the sudden increase of the thermal diffusivity which leads to a decrease in the temperature gradient. By comparing Fig. 19 and 23, it can be seen that for the same thickness of the insulations case 3 exhibits earlier occurrence of the temperature peak and also a greater value of it compared to case 5. It says that in the case of Ins1 more heat can penetrate faster into the wall.

Figure 23-26 show the variations of wall temperature vs crank angle and position for cases 5 and 6.

Figure 27 shows the outer wall heat flux for different cases. Case 2 lets more heat flux out of the wall and its related to its greater thermal diffusivity. In cases 3 and 4 and also in 5 and 6, increasing the insulation thickness lead to lower outer wall heat flux. Since, The ins2 has a low thermal diffusivity, it provides the least amount of heat rejection at the outer wall, even with lower thickness.

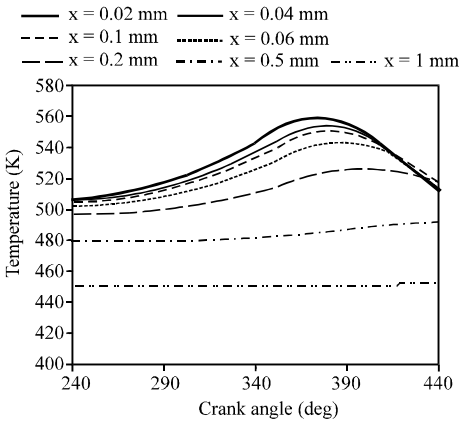

Fig. 21: Variation of wall temperature vs crank angle for different cylinder wall depth in cases 4

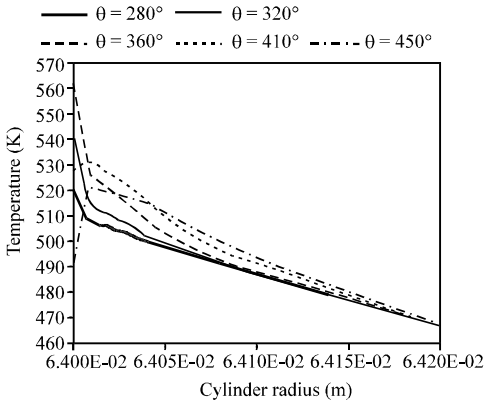

Fig. 24: Variation of wall temperature vs cylinder wall depth for different crank angles in case 5

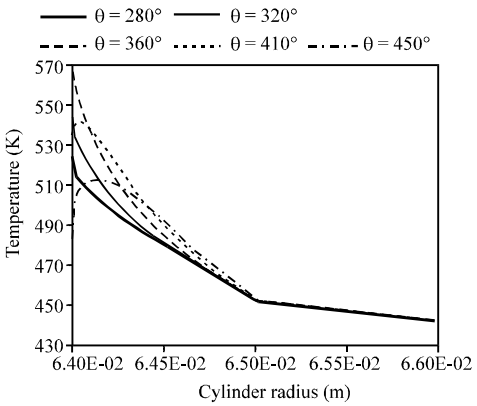

Fig. 22: Variation of wall temperature vs cylinder wall depth for different crank angles in case 4

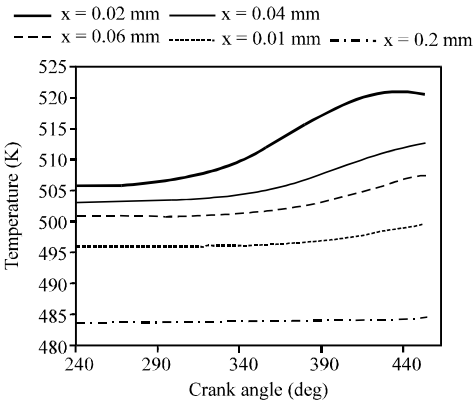

Fig. 25: Variation of wall temperature vs crank angle for different cylinder wall depth in case 6

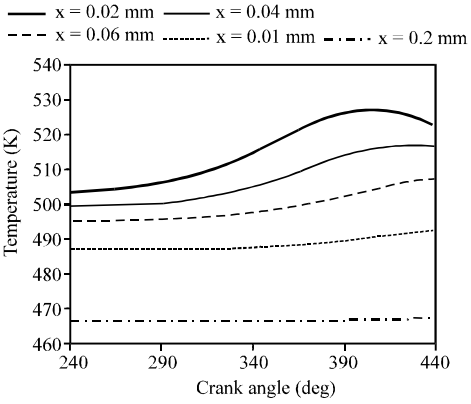

Fig. 23: Variation of wall temperature vs crank angle for different cylinder wall depth in case 5

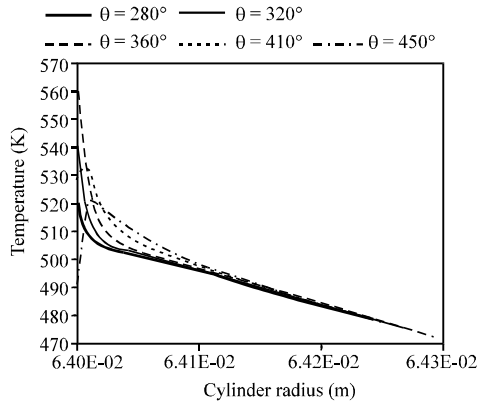

Fig. 26: Variation of wall temperature vs cylinder wall depth for different crank angles in case 6

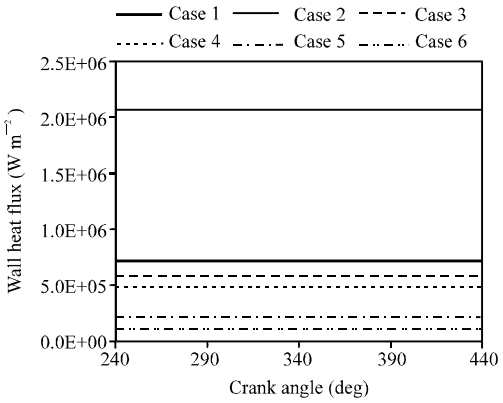

Fig. 27: Variation of outer wall heat flux for different cases

By decreasing the heat transfer from combustion chamber to the outer wall, more thermal efficiency can be achieved.

Main results: From this study, on the above mentioned cases on diesel engine modeling, the following conclusions may be drawn:

- The research demonstrated that the combination of multidimensional and analytical methods is useful for diesel engine wall heat transfer modeling.
- In the diagrams of temperature vs. crank angle, increase in depth led to a fall off and delay in temperature peak.
- In the diagrams of temperature vs. depth, increase in depth came along with damping of temperature oscillations and the temperature graphs came together after a distance. This distance was smaller for case 1 in comparison with case 2.
- Before TDC position, maximum temperature occurred on inner wall surface but after that it was somewhere inside the wall.
- Increasing the insulation thickness resulted in lower outer wall temperature and lower outer wall heat flux.

CONCLUSIONS

In the present study, the multidiensional combustion modeling was carried out for diesel engine. The numerical combustion simulations were done by the use of FIRE CFD tool. Also an analytical simulation was performed in order to investigate cylinder wall heat conduction. Analytical simulation was executed for six different cases of cylinder material and insulations. Numerical results were validated via experimental data for OM_355 DI diesel engine for mean cylinder pressure. There have been good agreements between experiments and the CFD calculations. For the purpose of achieving a low heat rejection condition from the above engine combustion chamber the effect of cylinder wall material, insulation material and thickness were studied. Alluminium chamber let more heat to the outer wall. But using cast iron as the cylinder material, along with the insulation coating on the inner wall reduced the outer wall temperature and heat flux noticeably.

NOMENCLATURE

U	=	Velocity (m sec^{-1})
P	=	Pressure (pa)
H	=	Enthalpy (J)
T	=	Temperature (K)
C	=	Species concentration (mol m^{-3})
k	=	Turbulent kinetic energy (m^2 sec^{-2})
m	=	Mass flow rate (kg sec^{-1})
Y	=	Mass fraction
c	=	Specific heat (J kg^{-1} K)
r_f	=	Stoichiometric coefficient
l_w	=	all thickness (m)
r	=	Cylinder wall radius (m)
ρ_r	=	Combustion reaction rate (kmol m^2 sec^{-1})
A_n and B_n	=	Fourier coefficients
q_w	=	Heat flux (W m^{-2})

Greek symbols

ρ	=	Density (kg m^{-3})
μ	=	Viscosity (kg m.sec^{-1})
λ	=	Thermal conductivity (W m.K^{-1})
ϕ	=	Equivalence ratio
ω	=	Combustion reaction rate (kmol m^2.sec)
ε	=	Turbulent dissipation rate (m^2 sec^{-3})
ω	=	Angular frequency (rad sec^{-1})
α	=	Thermal diffusivity (m^2 sec^{-1})

Subscripts

st	=	Stoichiometric
act	=	Actual
w	=	Wall
c	=	Coolant
p	=	Periodic

REFERENCES

Andreassi, L., S. Ubertini and L. Allocca, 2007. Experimental and numerical analysis of high pressure diesel spray-wall interaction. Int. J. Multiphase Flow, 33: 742-765.

Barata, J., 2008. Modelling of biofuel droplets dispersion and evaporation. J. Renewable Energy, 33: 769-779.

Baumgarten, C., 2006. Mixture Formation in Internal Combustion Engines. 1st Edn. Springer-Verlag Berlin Heidelberg, New York, ISBN: 103-540-30835-0 .

Brink, A., C. Mueller, P. Kilpinen and M. Hupa, 2000. Possibilities and limitations of the eddy break-up model. Combustion and Flame, 123: 275-279.

Burger, M., G. Klose, G. Rottenkolber, R. Schmehl and D. Giebert *et al*., 2002. A combined Eulerian and Lagrangian method for prediction of evaporating sprays. J. Eng. Gas Turbines Power, 142: 481-488.

Heywood, J.B., 1988. Internal Combustion Engine Fundamentals. 1st Edn. McGraw-Hill, New York, ISBN: 0-07-028637-X.

Liu, F.S., L. Zhou, B.G. Sun, Z.J. Li and H.J. Schock, 2008. Validation and modification of WAVE spray model for diesel combustion simulation. Fuel, 10.1016/j.fuel.2008.05.001.

Liu, Y. and R.D., Reitz, 1997. Multidimensional Modeling of Engine Combustion Chamber Surface Temperatures, SAE 971593. URL:http://www.sae.org/technical/papers/971593.

Mohammadi, A., M. Yaghoubi and M. Rashidi, 2008. Analysis of local convective heat transfer in a spark ignition engine. J. Int. Commun. Heat and Mass Transfer, 35: 215-224.

Pirouzpanah, V. *et al*., 2003. Reduction of pollutants emissions of OM_355 diesel engine to Euro 2 by convecting to dual fuel engine (diesel + gas). In: Proceeding of first conference of conversion automotive fuel to CNG, 19-20 June 2003, Tehran Iran, pp: 84-94.

Post, S.L. and J. Abraham, 2002. Modeling the outcome of drop-drop collisions in Diesel sprays. Int. J. Multiphase Flow, 28: 997-1019.

Rakopoulos, C.D., E.G. Giakoumis and D.C. Rakopoulos, 2004a. Cylinder wall temperature effects on the transient performance of a turbocharged diesel engine. J. Energy Conversion Manage., 45: 2627-2638.

Rakopoulos, C.D., D.C. Rakopoulos, G.C. Mavropoulos and E.G. Giakoumis, 2004b. Experimental and theoretical study of the short term response temperature transients in the cylinder walls of a diesel engine at various operating conditions. J. Applied Thermal Eng., 24: 679-702.

Rakopoulos, C.D. and G.C. Mavropoulos, 2008. Experimental evaluation of local instantaneous heat transfer characteristics in the combustion chamber of air-cooled direct injection diesel engine. Energy, 33: 1084-1099.

Sanli, A., A.N. Ozsezen, I. Kilicaslan and M. Canakci, 2008. The influence of engine speed and load on the heat transfer between gases and in-cylinder walls at fired and motored conditions of an IDI diesel engine. J. Applied Thermal Eng., 28: 1395-1404.

Torregrosa, A., P. Olmeda, B. Degraeuwe and M. Reyes, 2006. A concise wall temperature model for DI Diesel engines. J. Applied Thermal Eng., 26: 1320-1327.